SRTTU

JCARME
ISSN: 2228-7922
Journal of Computational and Applied Research in Mechanical Engineering
Vol. 9, No. 2, pp. 183-197
jcarme.sru.ac.ir

Effects of asymmetric behavior of shape memory alloy on nonlinear dynamic responses of thick sandwich plates with embedded SMA wires

A. Ghaznavi[a,*] and M. Shariyat[b]

[a] *Renewable Energies Department, Niroo Research Institute (NRI), Tehran, Iran*
[b] *Faculty of Mechanical Engineering, K.N. Toosi University of Technology, Tehran, Iran*

Article info:
Type: Research
Received: 04/09/2017
Revised: 17/02/2019
Accepted: 23/02/2019
Online: 25/02/2019

Keywords:
Higher-order global-local theory,
Nonlinear dynamic analysis,
Asymmetric behavior of SMA,
Finite element method.

Abstract
In the present article, the dynamic behavior of sandwich plates with embedded shape memory alloy (SMA) wires is evaluated for two cases wherein (i) the stress-strain curve of the superelastic behavior of the SMA wires is symmetric and (ii) the mentioned curve is non-symmetric. A modified version of Brinson's constitutive model is proposed and used. The high non-linearity in the behavior stems from the SMA wires embedded in the sandwich plate. In this regard, in addition to the proposed advanced algorithm for the determination of the martensite volume fraction, a Picard iterative solution algorithm is used in conjunction with Newmark's numerical time integration method for solving the resulting finite element equations. To improve the accuracy of the results, the variation of martensite volume fraction and material properties of individual points of the structure are updated continuously. Therefore, the kinetic equations of the phase transformation of the SMA are coupled with the motion equations, to accurately model the nonlinear behavior of the sandwich plate. For analysis of the thick sandwich plate, a higher-order global-local theory with novel 3D-equilibrium-based corrections is utilized. One of the features of this theory is the estimation capability of the nonlinear in-plane displacement components, and precise assessment of the transverse shear stresses through satisfying the continuity conditions of the shear stresses at the interfaces between layers. Another advantage of the proposed theory in comparison with the conventional approaches is the ability to simulate changes in the core thickness. This is especially important in cases where the core is relatively thick or soft.

Introduction

One of the most important features of the shape memory alloys (SMAs) is their remarkable deformation along with full retrieval capabilities. On the other hand, changes in the properties of such materials are due to their surrounding conditions, such as temperature and applied stresses. The combination of these properties has led to unique features in the shape-memory materials. For example, the formation of hysteresis loops under various loads, especially oscillating is one of the most important properties of SMAs.

[*] *Corresponding author*
email address: aghaznavi@nri.ac.ir

Different studies have been done to simulate the behavior of SMAs, and different models have been presented with different perspectives [1]. Although early researches on shape memory alloy reinforced composites (SMARCs) and shape memory alloy hybrid composites (SMAHCs) have been established by Roger and Robert [2], extensive developments have been done in these fields during the last decade. Some researchers [3] studied the use of these materials in constructional structures and buildings. Brinson and Lamring [4] presented a finite element code for studying the one-dimensional behavior of SMAs. Epps and Chandra [5] conducted analytical and laboratory research on composite beams with shape-memory wires. They used pre-tensioned SMA wires from the beginning. They tested the vibrations of the beam, despite the recovery stresses in the SMA wire. Lee et al. [6, 7] performed a numerical simulation of the thermal buckling behavior of composite shells with SMA wires using ABAQUS software. To simulate the thermomechanical behavior of the SMA wires, they wrote a fundamental equation for SMAs as a subroutine in ABAQUS. In general, it can be said that in many studies, several acceptable simplification approximations have been carried out to simulate the behavior of SMA wires. Lee et al. [8] studied the buckling and post-buckling behavior of SMA composites. They found that with the activation of SMA wires, the amount of buckling force of the composite sheet increases. Park et al. [9] investigated the vibrational behavior of composite sheets with the embedded SMA wires that are buckled with heat. They used nonlinear finite element equations based on the first-order shear theory. Ghomshei et al. [10] also studied the nonlinear finite element model for elastodynamic responses in composite beams with an SMA belt. To estimate the behavior of the beam, a higher-order theory was used. They used Brinson's one-dimensional fundamental model with sinusoidal kinetic phase transformation relations for simulation the SMA thermomechanical behavior. The numerical results indicated reducing effective vibration of the beam due to the activation of the pseudoelastic effect of SMA. Lu et al. [11] provided an analytical model for reinforced beams with SMA. The fundamental relations of the SMA layers were achieved using the micromechanical models.

Many papers have been published on the analysis of composite and sandwich plates, and various approaches have been proposed to model the behavior of these structures during the past decades. The main reason for the development of the two-dimensional plate theories is the serious difficulties exist in the 3D analysis of the plates, especially, the multi-layer ones. Different methods have been presented for reduction of the three-dimensional models of the multilayered composite plates to two-dimensional models through prescribing the transverse variations of the displacement components. Type of the transverse variations of the in-plane variables may be adopted according to one of the three general approaches of the [12] (i) equivalent single-layer theories, (ii) separate layers theory (layerwise theory), and (iii) theories based on the principle of superimposition (zigzag and global-local theories). One of the best methods for analyzing composite and sandwich plates is the use of global-local theories. The most efficient of these theories is the theory of superimposition principle because while maintaining the accuracy of the results due to a low number of variable parameters, it has a good performance in terms of run time. The basic idea of the theories based on superimposition rinciple is that a uniform displacement field is considered for all layers of multilayer or sandwich sheet (similar to the equivalent single-layer theory). Then, for examining different behaviors of the layers due to their different properties (zig-zag effect), independent displacement functions are considered for each layer. One of the studies carried out in this area was conducted by Cunningham et al. [13]. They investigated free vibrations of the sandwich plates through experiments and the finite element method. Tahani and Nosier [14] developed an elasticity formulation for general multi-layers plates under tension. Shariyat [15-17] presented a generalized higher-order global-local theory for studying bending and vibration of sandwich plates under thermomechanical loads. In this theory, the continuity conditions of the displacement components and transverse stresses between

layers, as well as the thickness change of the plate, were considered. One of the benefits of this theory is that the number of unknown parameters is independent of the number of layers. This theory can be considered as a generalized layerwise theory with considerable savings in computing time. The validity of the theory was confirmed by comparing the results of this theory with the results of the three-dimensional elasticity theory and the existing plate theories. Lezgy-Nazargah et al. [18] extended the previous work of Shariyat. Mantari and Soares [19] proposed modified higher-order shear-deformation finite element formulations for the bending analysis of multilayered sandwich and composite plates. In this modified higher-order theory, the number of degrees of freedom is limited by the number of independent layers.

In this paper, dynamic responses of sandwich plates under transverse loads is investigated. In order to induce structural damping and reduce the vibration amplitude, the sandwich plate face sheets are reinforced by SMA wires. In practice, majority of the shape memory materials have asymmetric behaviors in tension and compression; so that, identical martensite volume fractions are obtained at higher compression stresses in comparison to the tensile stresses, or as an example, the compressive recovery strain is less than that of the tensile one. As this behavior is more realistic and more compatible with practical examples, it can affect the global damping of sandwich plates reinforced by SMA wires. In the present research, the transverse flexibility of the core is also considered. A modified Brinson model, in addition to a proposed phase transformation algorithm, is used to simulate the behavior of SMA wires. Therefore, by providing this algorithm, it becomes possible to check the local loading and unloading event in different points of embedded SMA wires. In the following and before estimating the effects of different parameters on the sandwich plate behavior, verification of the written code for dynamic analysis, as well as the proposed algorithm for assessing SMA behavior, have been done with the available results of other references.

2. Development of the higher-order global-local governing equations of the sandwich plate with composite face sheets and embedded SMA wires

In order to study the behavior of shape memory wires in this paper, Brinson's constitutive model is slightly modified and used. The modification is implemented in both the constitutive law and the proposed phase transformation checking algorithm. According to this model, the stress-strain relationship in terms of the martensite volume fraction (ξ) is as follows:

$$\sigma - \sigma_0 = E(\xi)\varepsilon - E(\xi_0)\varepsilon_0 + \Omega(\xi)\xi_S - \Omega(\xi_0)\xi_{S0} \quad (1)$$

In Eq. (1), E is the elasticity modulus of the shape memory alloy mixture and Ω is the phase transformation function. The subscript "0" represents the initial condition of the material. Young's modulus is dependent on the volume fractions of the martensite and austenite volume fractions, as follow:

$$E = \xi E_m + (1-\xi)E_A \quad (2)$$

E_M and E_A are Young's moduli of the martensite and austenite phases, respectively. Brinson's model has two main problems:

(i) Eq. (1) is valid for the compressive stresses as well, only if the last two terms are multiplied by $\mathrm{sgn}(\sigma)$; an activity that is performed in the present research.

(ii) Concept of the ε_0 quantity must be redefined for the minor oscillations of the volume fraction of the martensite phase. In the present research, this quantity is updated in each global and local hysteresis loop.

Substantial relationships have been proposed to determine the volume fraction of martensite and SMA phase, and the relationships have been modified to allow the simulation of SMA behavior under compression loading. It should be mentioned that SMA wires are embedded in the middle plane of upper and lower of composite face sheets.

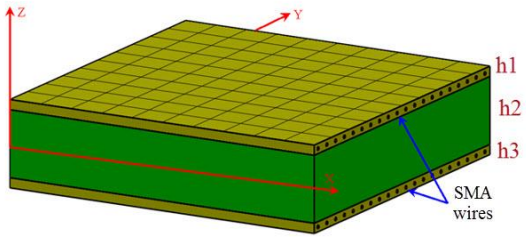

Fig. 1. Geometry and coordinate system of the sandwich plate with embedded SMA wires.

Length, width, and the total thickness of the studied sandwich plate are denoted by a, b, and H, respectively. The origin of the coordinate system is located on the middle plane and in the corner of the sandwich plate, and z-coordinate is supposed to be upward positive, as shown in Fig. 1. Thicknesses of the upper, core and lower layers are considered to be h1, h2 and h3, respectively. The upper and lower face sheets of the sandwich plate are reinforced by embedded SMA wires.

The displacement field of the kth-layer of the sandwich plate is considered to have both local and global variations:

$$\begin{cases} u^k(x,y,z) = u_G(x,y,z) + \\ \qquad u_L^k(x,y,z) \\ v^k(x,y,z) = v_G(x,y,z) + \\ \qquad v_L^k(x,y,z) \end{cases} \quad (3)$$

$$(k = 1,2,3)$$

in which u_G and v_G represent the global components of the displacement field of the sandwich plate and u_L and v_L show the local components of the displacement field. By applying the continuity condition of displacement components between different layers, the Eq. (3) is converted to:

$$\begin{cases} u^1 = u_0 + z\varphi_x + z^3\lambda_x(x,y,t) + \\ (z - z_1^u)\varphi_x^{(1)} + z_1^u\varphi_x^{(2)} \\ v^1 = v_0 + z\varphi_y + z^3\lambda_y(x,y,t) + \\ (z - z_1^u)\varphi_y^{(1)} + z_1^u\varphi_y^{(2)} \end{cases}$$

$$z_1^u \le z \le z_2^u$$

$$\begin{cases} u^2 = u_0 + z[\varphi_x + \varphi_x^{(2)}] + z^3\lambda_x(x,y,t) \\ v^2 = v_0 + z[\varphi_y + \varphi_y^{(2)}] + z^3\lambda_y(x,y,t) \end{cases}$$

$$z_1^l \le z \le z_1^u$$

$$\begin{cases} u^3 = u_0 + z\varphi_x + z^3\lambda_x(x,y,t) + \\ (z - z_1^l)\varphi_x^{(3)} + z_1^l\varphi_x^{(2)} \\ v^3 = v_0 + z\varphi_y + z^3\lambda_y(x,y,t) + \\ (z - z_1^l)\varphi_y^{(3)} + z_1^l\varphi_y^{(2)} \end{cases} \quad (4)$$

$$z_2^l \le z \le z_1^l$$

One of the distinguished hints of the present article is considering transverse variations of the lateral deflection in the core (Fig. 2).

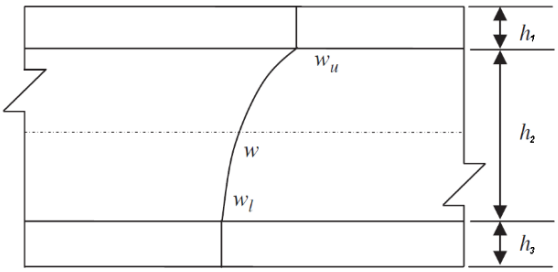

Fig. 2. Through thickness displacement.

Distribution of the transverse displacement $(\bar{W})$ of the core is considered as a quadratic function:

$$\begin{aligned} \bar{W} &= L_1 w_u + L_2 w + L_3 w, \\ L_1(z) &= z/h_2(1 + 2z/h_2), \\ L_2(z) &= 1 - 4z^2/h_2^2, \\ L_3(z) &= z/h_2(2z/h_2 - 1) \end{aligned} \quad (5)$$

where w_u, w_L and w are displacements of the top, bottom and the middle layers of the core, respectively, and L_1, L_2 and L_3 are quadratic Lagrange interpolation functions. Therefore, the 13 independent displacement parameters of the three-layer sandwich plate are as follows:

$$u_0, v_0, \varphi_x, \varphi_y, \lambda_x, \lambda_y, \varphi_x^{(1)}, \varphi_y^{(1)}, \varphi_x^{(2)}, \varphi_y^{(2)}$$
$$, \varphi_x^{(3)}, \varphi_y^{(3)}, w_u, w_m, w_l$$

The governing equations are extracted using Hamilton's principle. This principle is introduced in Eq. (5), in which U is the internal energy (strain), V is the work of the external forces, and K is kinetic energy:

$$\delta U - \delta W = 0 \tag{6}$$

$$\delta U = \int_A \int_{z_1^u}^{z_2^u} \begin{pmatrix} \sigma_{xx}^{(1)} \delta\varepsilon_{xx}^{(1)} + \sigma_{yy}^{(1)} \delta\varepsilon_{yy}^{(1)} + \\ \sigma_{zz}^{(1)} \delta\varepsilon_{zz}^{(1)} + \sigma_{xy}^{(1)} \delta\gamma_{xy}^{(1)} + \\ \sigma_{xz}^{(1)} \delta\gamma_{xz}^{(1)} + \sigma_{yz}^{(1)} \delta\gamma_{yz}^{(1)} \end{pmatrix} dz\, dA$$
$$+ \int_A \int_{z_1^l}^{z_1^u} \begin{pmatrix} \sigma_{xx}^{(2)} \delta\varepsilon_{xx}^{(2)} + \sigma_{yy}^{(2)} \delta\varepsilon_{yy}^{(2)} + \\ \sigma_{zz}^{(2)} \delta\varepsilon_{zz}^{(2)} + \sigma_{xy}^{(2)} \delta\gamma_{xy}^{(2)} + \\ \sigma_{xz}^{(2)} \delta\gamma_{xz}^{(2)} + \sigma_{yz}^{(2)} \delta\gamma_{yz}^{(2)} \end{pmatrix} dz\, dA \tag{7}$$
$$+ \int_A \int_{z_2^l}^{z_1^l} \begin{pmatrix} \sigma_{xx}^{(3)} \delta\varepsilon_{xx}^{(3)} + \sigma_{yy}^{(3)} \delta\varepsilon_{yy}^{(3)} + \\ \sigma_{zz}^{(3)} \delta\varepsilon z_{zz}^{(3)} + \sigma_{xy}^{(3)} \delta\gamma_{xy}^{(3)} \\ + \sigma_{xz}^{(3)} \delta\gamma_{xz}^{(3)} + \sigma_{yz}^{(3)} \delta\gamma_{yz}^{(3)} \end{pmatrix} dz\, dA$$

$$\delta W = \int_A q \delta\bar{W}\, dA -$$
$$\int_A \int_z \rho(u\, \delta\ddot{u} + v\, \delta\ddot{v} + w\, \delta\ddot{w}) dz dA$$

$$= \int_A q \delta\bar{W}\, dA - \int_A \{ \int_{z_1^u}^{z_2^u} \rho_1 (u_1 \delta\ddot{u}_1 + v_1 \delta\ddot{v}_1 + w_1 \delta\ddot{w}_1) dz \tag{8}$$
$$+ \int_{z_1^l}^{z_1^u} \rho_2 (u_2 \delta\ddot{u}_2 + v_2 \delta\ddot{v}_2 + w_2 \delta\ddot{w}_2) dz$$
$$+ \int_{z_2^l}^{z_1^l} \rho_3 (u_3 \delta\ddot{u}_3 + v_3 \delta\ddot{v}_3 + w_3 \delta\ddot{w}_3) dz \} dA$$

In calculating the stiffness of each layer, the properties of the composite layer with SMA wires are calculated by the following relationships [20]:

$$E_l(\xi) = E_l^c k_c + E_s(\xi) k_s \tag{9}$$
$$E_t(\xi) = E_t^c / (1 - \sqrt{k_s}(1 - E_t^c / E_s(\xi))) \tag{10}$$
$$G_{lt}(\xi) = G_{lt}^c G_s(\xi) / (k_c G_s(\xi) + k_s G_{lt}^c) \tag{11}$$
$$\upsilon_{lt} = \upsilon_{lt}^c k_c + \upsilon_s k_s \tag{12}$$

In the above relations, the *s* and *c* subscripts represent SMA and composite, respectively. Based on Eqs. (1 and 9-12) the strain-stress relation for a layer with SMA wires is:

$$\begin{bmatrix} \sigma_1 \\ \sigma_2 \\ \sigma_3 \\ \sigma_4 \\ \sigma_5 \\ \sigma_6 \end{bmatrix} = \begin{bmatrix} C_{11} & C_{12} & C_{13} & 0 & 0 & 0 \\ C_{12} & C_{22} & C_{23} & 0 & 0 & 0 \\ C_{13} & C_{23} & C_{33} & 0 & 0 & 0 \\ 0 & 0 & 0 & C_{44} & 0 & 0 \\ 0 & 0 & 0 & 0 & C_{55} & 0 \\ 0 & 0 & 0 & 0 & 0 & C_{66} \end{bmatrix} \begin{bmatrix} \varepsilon_1 \\ \varepsilon_2 \\ \varepsilon_3 \\ \varepsilon_4 \\ \varepsilon_5 \\ \varepsilon_6 \end{bmatrix} - \begin{bmatrix} k_s E_s \zeta \varepsilon_L \\ 0 \\ 0 \\ 0 \\ 0 \\ 0 \end{bmatrix} \tag{13}$$

in which, k_s and E_s are martensite volume fraction and Young's modulus of the SMA, respectively. It is worth mentioning that these parameters are variable for different layers, different points of the layers, and they can vary over time. These conditions have made the solution more complicated. In this equation; the stiffness of *k*th-layer form composite shell with embedded SMA wires is C_{ij}^k. Eq. (14) can be rewritten in the presence of SMA wires in the following form:

$$\boldsymbol{\sigma} = \boldsymbol{C}\varepsilon - \boldsymbol{\sigma}^s \tag{14}$$

and:

$$\int_{z_1^u}^{z_2^u} \sigma_{ij} \begin{Bmatrix} 1 \\ z \end{Bmatrix} dz = \begin{Bmatrix} N_{ij}^{(1)} \\ M_{ij}^{(1)} \end{Bmatrix} - \begin{Bmatrix} N_{ij}^{(1)} \\ M_{ij}^{(1)} \end{Bmatrix}^S,$$
$$\int_{z_1^l}^{z_1^u} \sigma_{ij} \begin{Bmatrix} 1 \\ z \end{Bmatrix} dz = \begin{Bmatrix} N_{ij}^{(2)} \\ M_{ij}^{(2)} \end{Bmatrix},$$
$$\int_{z_2^l}^{z_1^l} \sigma_{ij} \begin{Bmatrix} 1 \\ z \end{Bmatrix} dz = \begin{Bmatrix} N_{ij}^{(3)} \\ M_{ij}^{(3)} \end{Bmatrix} - \begin{Bmatrix} N_{ij}^{(3)} \\ M_{ij}^{(3)} \end{Bmatrix}^S,$$

(i, j= x,y,z)

$$\int_{z_1^u}^{z_2^u} \sigma_{kz} \begin{Bmatrix} 1 \\ z \\ z^2 \end{Bmatrix} d = \begin{Bmatrix} P_k^{(1)} \\ Q_k^{(1)} \\ R_k^{(1)} \end{Bmatrix},$$

$$\int_{z_1^u}^{z_1^l} \sigma_{kz} \begin{Bmatrix} 1 \\ z \\ z^2 \end{Bmatrix} dz = \begin{Bmatrix} P_k^{(2)} \\ Q_k^{(2)} \\ R_k^{(2)} \end{Bmatrix}, \quad (15)$$

$$\int_{z_2^l}^{z_1^l} \sigma_{kz} \begin{Bmatrix} 1 \\ z \\ z^2 \end{Bmatrix} dz = \begin{Bmatrix} P_k^{(3)} \\ Q_k^{(3)} \\ R_k^{(3)} \end{Bmatrix}, \text{ (k= x,y)}$$

where:

$$\begin{Bmatrix} N_{xx}^S \\ N_{yy}^S \\ N_{xy}^S \end{Bmatrix}^{(1)} =$$

$$\int_{z_1^u}^{z_2^u} \begin{Bmatrix} k_s^{(1)} E_s^{(1)} \xi^{(1)} \varepsilon_L \cos^2(\theta^{(1)}) \\ k_s^{(1)} E_s^{(1)} \xi^{(1)} \varepsilon_L \sin^2(\theta^{(1)}) \\ k_s^{(1)} E_s^{(1)} \xi^{(1)} \varepsilon_L \sin(\theta^{(1)}) \cos(\theta^{(1)}) \end{Bmatrix} dz,$$

$$\begin{Bmatrix} M_{xx}^S \\ M_{yy}^S \\ M_{xy}^S \end{Bmatrix}^{(1)} =$$

$$\int_{z_1^u}^{z_2^u} \begin{Bmatrix} k_s^{(1)} E_s^{(1)} \xi^{(1)} \varepsilon_L \cos^2(\theta^{(1)}) \\ k_s^{(1)} E_s^{(1)} \xi^{(1)} \varepsilon_L \sin^2(\theta^{(1)}) \\ k_s^{(1)} E_s^{(1)} \xi^{(1)} \varepsilon_L \sin(\theta^{(1)}) \cos(\theta^{(1)}) \end{Bmatrix} zdz \quad (16)$$

$$\begin{Bmatrix} N_{xx}^S \\ N_{yy}^S \\ N_{xy}^S \end{Bmatrix}^{(3)} =$$

$$\int_{z_1^l}^{z_2^l} \begin{Bmatrix} k_s^{(3)} E_s^{(3)} \xi^{(3)} \varepsilon_L \cos^2(\theta^{(3)}) \\ k_s^{(3)} E_s^{(3)} \xi^{(3)} \varepsilon_L \sin^2(\theta^{(3)}) \\ k_s^{(3)} E_s^{(3)} \xi^{(3)} \varepsilon_L \sin(\theta^{(3)}) \cos(\theta^{(3)}) \end{Bmatrix} dz,$$

$$\begin{Bmatrix} M_{xx}^S \\ M_{yy}^S \\ M_{xy}^S \end{Bmatrix}^{(3)} =$$

$$\int_{z_2^l}^{z_1^l} \begin{Bmatrix} k_s^{(3)} E_s^{(3)} \xi^{(3)} \varepsilon_L \cos^2(\theta^{(3)}) \\ k_s^{(3)} E_s^{(3)} \xi^{(3)} \varepsilon_L \sin^2(\theta^{(3)}) \\ k_s^{(3)} E_s^{(3)} \xi^{(3)} \varepsilon_L \sin(\theta^{(3)}) \cos(\theta^{(3)}) \end{Bmatrix} zdz$$

If the solution domain is discretized by rectangular elements, through the shape functions matrix $\mathcal{N}$:

$$\begin{aligned} \boldsymbol{\varphi} &= \left\langle u_0, v_0, \varphi_x, \varphi_y, \lambda_x, \lambda_y, \varphi_x^{(1)}, \varphi_y^{(1)}, \right. \\ &\left. \varphi_x^{(2)}, \varphi_y^{(2)}, \varphi_x^{(3)}, \varphi_y^{(3)}, w_u, w_m, w_l \right\rangle^T \\ &= \mathcal{N}\Phi^{(e)} \\ \varepsilon &= \Lambda\Phi^{(e)} \\ \sigma &= \mathcal{C}\Lambda\Phi^{(e)} \end{aligned} \quad (17)$$

Eqs. (6-8) may be rewritten as:

$$\begin{aligned} \delta U &= \int_\Omega (\delta\varepsilon)^T \sigma d\Omega = \\ &\int_\Omega (\delta\Phi^{(e)})^T \Lambda^T (\mathcal{C}\Lambda\Phi^{(e)} - \sigma^s) d\Omega \end{aligned} \quad (18)$$

$$\begin{aligned} \delta V &= -\int_A q \delta w_u dA = \\ &\int_A q (\delta\Phi^{(e)})^T (R\mathcal{N})^T dA, \end{aligned} \quad (19)$$

$$R = [\mathbf{0} \quad \mathbf{0} \quad \mathbf{1}]$$

$$\begin{aligned} \delta K &= -\int_\Omega \rho (\delta\Phi^{(e)})^T \ddot{\Phi} d\Omega = \\ &-\int_\Omega \rho (\delta\Phi^{(e)})^T \mathcal{N}^T \mathcal{N} \ddot{\Phi}^{(e)} d\Omega \end{aligned} \quad (20)$$

Finally, by inserting the above relations in the Hamilton principle (Eq. (6)), the SMA effect appears, the following equation is obtained:

$$\begin{aligned} (\delta\Phi^{(e)})^T [&\int_\Omega \rho \mathcal{N}^T \mathcal{N} \ddot{\Phi}^{(e)} d\Omega \\ &+ \int_\Omega \Lambda^T \mathcal{C} \Lambda \Phi^{(e)} d\Omega \\ &- \int_\Omega \Lambda^T \sigma^s d\Omega - \int_A q (R\mathcal{N})^T dA] = 0 \end{aligned} \quad (22)$$

It is possible to transfer all terms with SMA origin of the equation to one side of the equation and include them in a unitary force vector. On

the other hand, since the above equation holds for any arbitrary $\delta\Phi^{(e)}$, the following governing equation of motion can be reached:

$$\mathbf{M}\ddot{\mathbf{\Phi}} + [\mathbf{K}(\mathbf{\Phi})]\mathbf{\Phi} = [\boldsymbol{F}(\mathbf{\Phi})] \quad (23)$$

where K is the matrix of stiffness, M is the mass matrix, and F is the force matrix. It should be noted that in Eq. (24), the stiffness and force matrices are functions of the martensite volume fraction. The martensite volume fraction, in turn, changes instantaneously and locally in different points and layers of the face sheet and is itself a function of displacements of the Gaussian points. To solve Eq. (23), the finite element method based on nonlinear rectangular elements has been used.

3. Solving the nonlinear dynamic finite element equations

For the time discretization of the nonlinear dynamic Eq. (24), Newmark's method is used as follows [21]:

$$\mathbf{\Phi}_{m+1} = \mathbf{\Phi}_m + \Delta t\ \dot{\mathbf{\Phi}}_m + 1/2\,\Delta t^2\ \ddot{\mathbf{\Phi}}_{m+\gamma} \quad (24)$$

$$\dot{\mathbf{\Phi}}_{m+1} = \dot{\mathbf{\Phi}}_m + \Delta t\ \mathbf{\Phi}_{m+\alpha} \quad (25)$$

where Δt, $\mathbf{\Phi}$ and $\dot{\mathbf{\Phi}}$ are the time increment, displacement vector and time derivative of the displacement vector, respectively. Also, the subscript *m* shows the time step number and $\alpha = 1/2$ and $\gamma = 8/5$. The acceleration of $\ddot{\mathbf{\Phi}}_{m+\gamma}$ can be written as a linear combination of acceleration of steps *m* and *m+1*:

$$\ddot{\mathbf{\Phi}}_{m+\gamma} = (1-\gamma)\ddot{\mathbf{\Phi}}_m + \gamma\ddot{\mathbf{\Phi}}_{m+1} \quad (26)$$

Using Eqs. (23 and 24), Eq. (22) can be expressed as follow:

$$\hat{K}_{m+1}\mathbf{\Phi}_{m+1} = \hat{F}_{m+1} \quad (27)$$

where

$$\hat{K}_{m+1} = K_{m+1} + a_3 M \quad (28)$$

$$\hat{F}_{m+1} = F_{m+1} + M(a_3\mathbf{\Phi}_m + a_4\dot{\mathbf{\Phi}}_m + a_5\ddot{\mathbf{\Phi}}_m) \quad (29)$$

and the coefficients a_3, a_4, and a_5 are defined as:

$$\begin{aligned} a_3 &= 2/(\gamma(\Delta t)^2), \\ a_4 &= 2/(\gamma\Delta t), \\ a_5 &= 1/\gamma - 1 \end{aligned} \quad (30)$$

The initial acceleration value is usually unknown. As an estimate, the initial acceleration can be calculated using the above relation and the initial values of $\mathbf{\Phi}_0$ and F_0 (F_0 is usually considered as zero) are calculated as follows:

$$\ddot{\mathbf{\Phi}}_0 = M^{-1}(F_0 - K\mathbf{\Phi}_0) \quad (31)$$

At the end of each time step, the acceleration and velocity values are calculated using the following relations:

$$\ddot{\mathbf{\Phi}}_{m+1} = a_3(\mathbf{\Phi}_{m+1} - \mathbf{\Phi}_m) - a_4\dot{\mathbf{\Phi}}_m - a_5\ddot{\mathbf{\Phi}}_m \quad (32)$$

$$\dot{\mathbf{\Phi}}_{m+1} = \dot{\mathbf{\Phi}}_m + a_2\ddot{\mathbf{\Phi}}_m + a_1\ddot{\mathbf{\Phi}}_{m+1} \quad (33)$$

where $a_1 = \alpha\Delta t$ and $a_2 = (1-\alpha)\Delta t$.

Also, for solving nonlinear equations, an iterative method is suggested with the following steps:

1. Defining the initial values for $\dot{\mathbf{\Phi}}_0, \mathbf{\Phi}_0$ and ζ_0^k (that are usually considered as zero),
2. Calculating initial acceleration value $\ddot{\mathbf{\Phi}}_0$,
3. Determining new time step $t_{m+1} = t_m + \Delta t_{m+1}$ and calculating the new martensite volume fractions,
4. Calculating the material properties of each layer and material properties of the whole sandwich and then obtaining the stiffness matrix based on the calculated martensite volume fraction in the new time step; this is the major source of the nonlinearity of the problem. In other words, the formation of stiffness matrix in the mth time step is based on the existing results for displacement and martensite volume fraction in (m-1)th time step. It should be mentioned that in this issue, every point of the plate is investigated

completely independently. In other words, the behavior of various points of SMA wires is different in various parts of the sandwich plate, such that part of the plate and consequently the SMA wire can be in the position of loading, whereas another point of the plate and SMA wires can be in the position of unloading. This is important because the suggested algorithm for estimating shape memory alloy behavior in both loading and unloading positions is entirely different which increases the complicatedness of the issue. Another complexity of this issue is that in some cases, after changing the direction of the applied load on shape memory alloy, many of parameters have to be updated including martensite initial volume fraction, etc. While in some cases, this update should not be done. The matter whether in what cases initial parameters have to be updated and in what cases they do not change was fully explained in Ref [21-23]. An algorithm is provided to accurately investigate the behavior of shape memory alloy which is regarded as the basis of the written code to study the behavior of this material while considering all mentioned issues. Based on this algorithm, in every time increment, it should first be determined that the imposed force is tension or compression in the intended gauss point and that whether SMA wires are in the loading or unloading and then it should be investigated that which level of phase transformation is occurring. It is possible that, due to dynamic loading and also considering the continuity of the mentioned SMA wires, in some of time increment in some parts of the plate local loading-unloading takes place or in cases in which a part of the plate is under compression load, the other part of it is under tension load which leads to the higher complicatedness of sandwich plate with composite face sheet embedded SMA wires.

5. Solving Eq. (22) to obtain $\mathbf{\Phi}_{m+1}^{k}$,
6. Examining convergence of the results at any time step with the following criteria:

$$\left\|\mathbf{\Phi}_{m+1}^{(k+1)}-\mathbf{\Phi}_{m+1}^{(k)}\right\| \Big/ \left\|\mathbf{\Phi}_{m+1}^{(k+1)}\right\| \cong \in \qquad (34)$$

where *k* represents the number of iteration of the (m+1)th time step and $\in$ is a very small number. In the case of convergence, different components of the stress and strain of the plate and SMA wires and martensite volume fraction of SMA wires are calculated for different points of the plate and a time step is added to the problem solution until achieving to the final time of the solution. It should be noted that a proposed dynamic phase transformation algorithm is used to calculate the martensite volume fraction. By using the proposed algorithm, the status of SMA wires (loading and unloading and other parameters) at each time step is determined in each gauss point independently; and then, it is assessed by the algorithm to determine the situation of the phase transformation. It should be noted that because of the thickness of the sandwich plate and type of applied load; it is likely that a lot of loading/unloading in different points of the plate occurs at the same time or among different time steps.

4. Results and discussion

4.1. Verification and mesh independency

Initially, before investigating the behavior of the sandwich plate and the effects of various parameters on its behavior, the correctness of the proposed algorithm and the written code are examined. In order to prove the correctness; at first, the behavior of SMA is studied under various cyclic loadings and then, the results are compared with experimental results in the literature. Cyclic loading is chosen because, in reality, points of the plate are under fluctuating loads. The proposed algorithm for simulating the SMA behavior should have the ability to consider several loading and unloading during all stages of the phase transformation in different locations.

Variation of stress under constant temperature is one of the most important load cases in SMA. The response of the SMA to the mentioned cyclic load is shown in Fig. 3 and compare with the experimental result. As can be seen, the excellent matching of the obtained result from the written code and the results of the experimental tests [24] are obvious. Second, the mesh independency of the obtained results

should be checked. For this reason, plates are meshed using various numbers of the 2D quadratic nonlinear element with 8 nodes such as 5 × 5, 10 × 10, 20 × 20, 30 × 30 and 40 × 40, and their results are examined. The obtained results are analyzed for the thick plates with a/h ratio of 4. Various results such as non-dimensional transverse stresses and dimensionless transverse displacement are investigated. Fig. 4 also shows the convergence of the results for dimensionless transverse shear stresses. As can be seen, the results of most transverse shear stresses with the element size of 40 ×40 converge. In the case of a square plate, the number of elements in the length and width of the plate is equal. Verification of the converged results is presented in Table 1. Ref. [25-27] are used for this verification.

Finally, the obtained results showed that the mesh size 40 × 40 led to the provision of converged results, and the further increase in sandwich plate elements did not have a significant effect on the results. Also, comparing the obtained results with those existing in Ref. [28] made it clear that the theory has an acceptable accuracy. The obtained results are compared with the three-dimensional result of the elasticity existing in Ref. [29]. The investigations showed that for a thick sandwich plate, the results calculated by the proposed theory are acceptable and have very good accuracy. More verification of the converged results is presented in Table 1. The obtained results are compared with the three-dimensional result of the elasticity existing in Refs. [26-28].

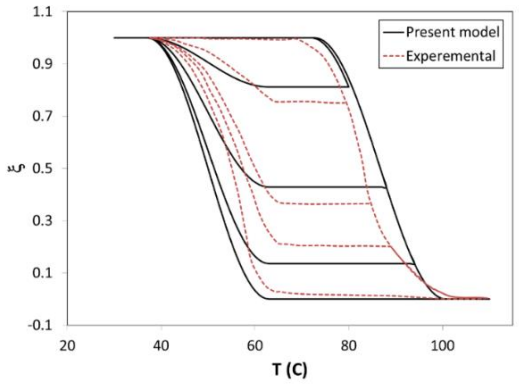

Fig. 3. Obtained result by proposed algorithm and implemented code and experimental result [24] of SMA under a cyclic load.

Table 1. The results of dimensionless interlaminate shear stresses of sandwich plate with soft core for different mesh sizes.

a/h		Pagano[25]	Sheikh[26]	Cho [27]
4	S_{xz} (L/2,0,0)	0.256	0.2023	**0.238***
	S_{yz} (0,L/2,0)	0.2172	0.1831	**0.229***
	S_{zz} (L/2,L/2,0)	0.4926	—	**0.498***
a/h		**Present Stud0y (Mesh density)**		
		16×16	30×30	**40×40**
4	S_{xz} (L/2,0,0)	0.2706*	0.2557*	**0.2515***
	S_{yz} (0,L/2,0)	0.2258*	0.2185*	**0.2180***
	S_{zz} (L/2,L/2,0)	0.553	0.5373	**0.5152**

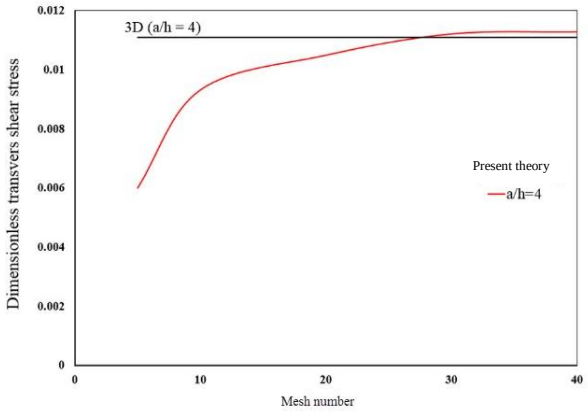

Fig. 4. Mesh independency of the dimensionless transverse shear stress for thick sandwich plate (a/h=4).

Also, in order to ensure the function of the written code, the dynamic analysis of the three-layer composite plate is compared with the results presented by Khadeir and Reddy [29]. They studied dynamic responses of a symmetric cross-ply laminated composite using a high-order shear-deformation theory. The properties of the layers considered in this analysis are:

$E_1 = 172.369GPa$, $G_{12} = G_{13} = 3.448\ GPa$,
$v_{12} = 0.25$, $E_2 = 6.895\ GPa$, $G_{23} = 1.379\ GPa$,
$\rho = 1603.03\ kg/m^3$

A sinusoidal load is imposed in a short time (as a pulse) on the top of the composite plate. Fig. 5 shows the transverse displacement of the middle point of the plate after applying the dynamic load. In this figure, the result obtained from the presented formulation and the result of the mentioned reference are shown simultaneously. As can be seen, the obtained results are consistent with that provided in Ref. [29].

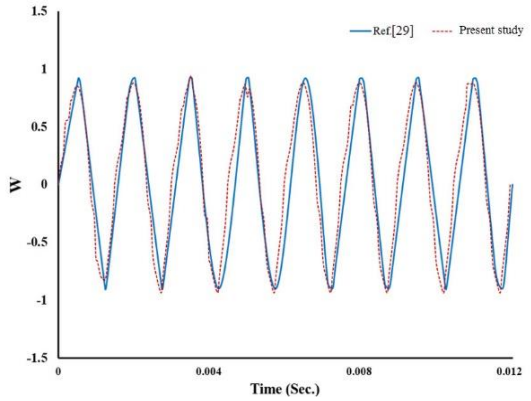

Fig. 5. A comparison between time histories of the lateral deflection of the central point of the plate predicted by present approach and Ref. [29] for a three-layer composite plate under an impulse load.

4.2. Influence of the SMA behavior of the dynamic response of thick sandwich plate with embedded SMA wires

In this section, the effects of the SMA wires behavior on the performance of the sandwich plate are studied. Results are obtained for a square simply-supported sandwich plate whit 0.1h face sheets thickness and 0.8 h core thickness and for thick (*a/h=4*) sandwich plates with very soft ($E_f/E_c=10^5$) cores. The sandwich plate is subjected to a uniform step impulse pressure that is applied to the top surface of the sandwich plate. Due to applying loads in a very short time, the plate fluctuates around a non-zero displacement. The SMA wires are embedded in the middle layer of the upper and lower composite face sheets of the sandwich plate with a volume fraction of 50%. The mechanical properties of the SMA used in the nonlinear analysis are given in Table 2. While symmetric behavior is considered, the compression properties are considered completely equal to the tensile properties of Table 2. Since the main purpose of this paper is to investigate the effect of the SMA wires and its behavior on the damping of the sandwich plate, the amount of applied load is chosen so that SMA wires enter the phase transformation range and can be able to absorb some part of the energy of the sandwich structure. The following dimensionless displacement parameter is defined to extract the results:

$$W = w\frac{100E_2^{skin}h^3}{a^4q_0}$$

Fig. 6 shows time histories of the dimensionless transverse displacement (*W*) of the central point of the upper and lower face sheets of the thick sandwich plate with a soft core. Fig. 6(a) shows the dynamic response of the sandwich with the embedded SMA wires that act completely the same in the compression and tension. And, the behavior of embedded SMA wires is asymmetric in Fig. 6(b). Due to the thickness of the sandwich and stiffness of the core, the difference between displacement amplitude of the top and bottom layers is a lot. In other words, when the upper layer displaces in a significant amount because of the applied load, the lower layer is not significantly influenced by the applied load to the upper layer.

Table 1. Mechanical properties of the SMA [30].

$E_A = 33000MPa$	$M_f = 5^\circ C$
$E_M = 18300MPa$	$M_s = 10^\circ C$
$\upsilon = 0.33$	$\rho = 6500\ kg/m^3$
$C_A^+ = 8\ MPa/^\circ C$	$\sigma_s^{cr,+} = 40\ MPa$
$\varepsilon_L^+ = 0.08$	$C_M^- = 8.4MPa/^\circ C$
$\sigma_s^{cr,-} = 51.8MPa$	$\sigma_f^{cr,-} = 110.6MPa$
$A_s = 28^\circ C$	$\sigma_f^{cr,+} = 80\ MPa$
$A_f = 32^\circ C$	$C_A^- = 11.2MPa/^\circ C$
$C_M^+ = 6\ MPa/^\circ C$	$\varepsilon_L^- = 0.06$

Thus, the difference in the range of oscillation in both layers is very significant. Furthermore, it is shown in Fig. 6 that when the behavior of the SMA wires is symmetrical, the sandwich plate in the upper layer experiences more dimensionless

transverse displacements in comparison to the case with the asymmetric behavior of the SMA wires. The symmetric behavior of the SMA wires means that the phase transformation in the compression stress occurs at the same level as the tension one. So it leads to starting the phase transformation at the lower level of stress in comparing to the unsymmetrical case.

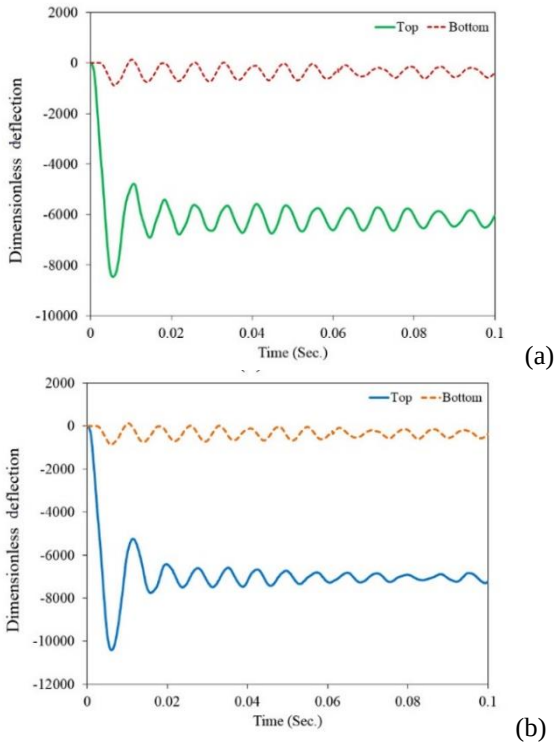

Fig. 6. Time histories of the dimensionless transverse displacements of the central points of the top and bottom layer of the thick sandwich plate with a very soft core; (a) unsymmetrical behavior of embedded SMA and (b) symmetrical behavior of embedded SMA.

Considering this fact that during the phase transformation, Young's modulus of the SMA wires decreases; it is completely reasonable that symmetric behavior of the SMA leads to pronounced reductions in the plate stiffness in lower stress level, and as a result, to an increased amplitude of the transverse vibration. Of course, since the bottom layer is not affected by the applied load impressively, embedded SMA wires of the bottom layer has not experienced phase transformation; for this reason, there is practically no difference between the two responses.

Fig. 7 shows the changes in the martensite volume fraction of the embedded SMA wires located in the middle of the upper and lower composite face sheets over time. As can be seen, if the SMA wires behavior in tension and compression is nonsymmetric, martensite volume fraction converges to 100% after a few cycles and during the rest of the analysis, SMA wires vibrate in the complete martensite phase. However, in the other case (symmetrical behavior of the SMA), the martensite volume fraction needs more cycles for convergence and eventually reaches to a number other than a convergent one.

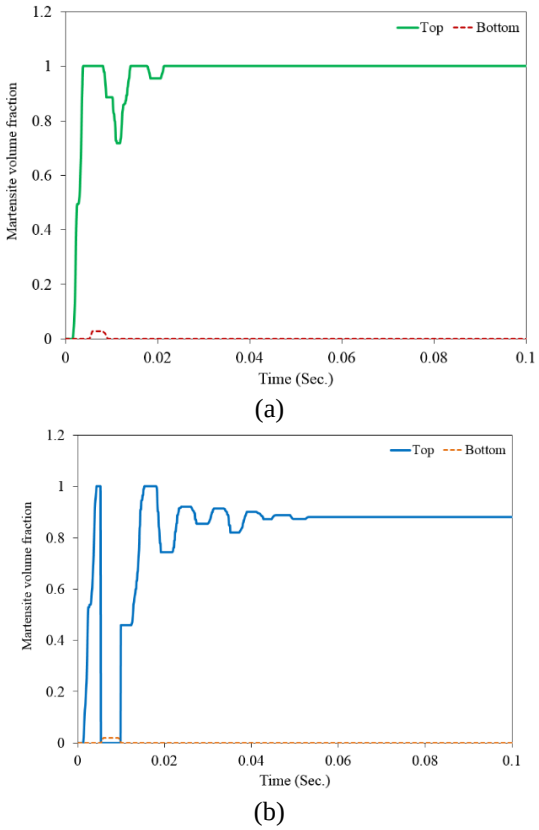

Fig. 7. Time history of martensite volume fraction of central point of the embedded SMA wires in top and bottom layers; (a) unsymmetrical behavior of SMA and (b) symmetrical behavior of SMA.

In this case, the embedded SMA wires remain in the phase transformation stage, in other words, the SMA wires remain active in damping of the stored energy of the sandwich structure, in

contrast to the first sample (unsymmetrical behavior) wherein the SMA wires lose their damping ability after a few cycles.

Fig. 8 shows the hysteresis loop formed at the embedded SAM wire in the midpoint of the upper composite face sheet. In this figure, the dynamic response of the SMA wires with both assumption (symmetrical and unsymmetrical behavior of shape memory alloy) is investigated. Since the applied load is a step, the sandwich panel remains under continuous pressure after loading process and as a consequence the SAM wires embedded in the top face sheet vibrate under compression and with the negative stress and strain.

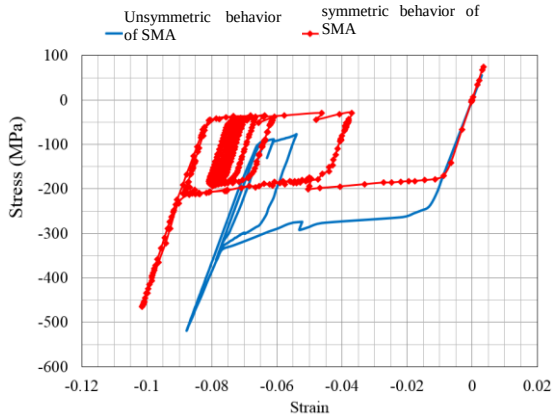

Fig. 8. Hysteresis loop for embedded SMA wires in the top layer of thick sandwich with the soft core.

This is important because as mentioned earlier, the difference between symmetrical and unsymmetrical assumption is only observed in compression, not in tension. Since the embedded SMA wires in the top layer are in the compression throughout the analysis, the noted difference in the energy assumption may readily be noted. The recovery strain in a sample in which the SMA behavior is non-symmetrical is less than that with symmetrical behavior. This difference between the amounts of the recovery strains could be the major reason for the phase shifts of responses of the SMA wires at the final time instant of solution. In the anisotropic SMA (realistic), the behavior of SMA in compression is deferent from the tension. In other words, in the anisotropic SMA, *MS s-*, *MF s-*, *AS s-* and *AF s-* are larger than *MS s+*, *MF s+*, *AS s+ and AF s+*, but in the symmetric manner of SMA, these critical points are the same. So because of this difference between starting and finishing point of phase transformation, in an unsymmetrical manner, the SMA wire becomes completely martesite but in the symmetrical case phase transformation in the reverse direction start and SMA wires are not complete in the martensite phase, and become a combination of martensite and austenite.

As can be seen in Figs. 7 and 8, for the case associated with unsymmetrical phase transformation, the SMA wires become pure martensite at the end of solution, but for the other case, the SMA wires contain both the martensite and austenite phases, although the resulting mixture is very close to the martensite phase and converges to a martensite volume fraction of 0.9. Also, the difference between the beginning stresses of phase transformation is noticeable in the two responses. In addition, local loading and unloading are also observed during the phase transformation (martensite to austenite or vice versa) in the hysteresis loop which can be due to various reasons, including the uniformity of frequency with the natural frequency of the sandwich plate, especially in higher modes. 3D plots of martensite volume fractions of the SMA wires at the midpoint of the upper layer of the thick sandwich plate with the soft core are shown in Fig. 9, for the first peaks of Fig. 6.

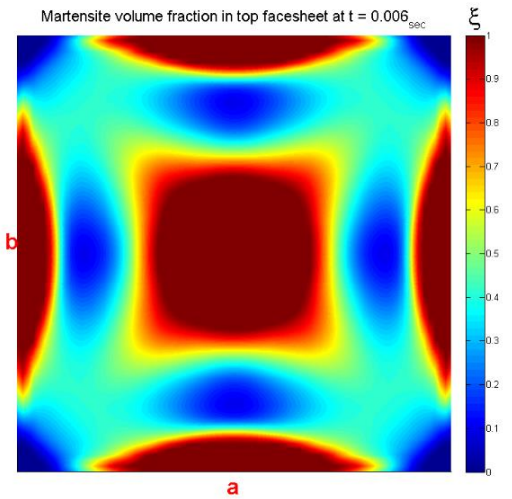

Fig. 9. 3D Plots for in-plane distributions of the martensite volume fraction at the midpoint of the upper layer of a thick plate with a flexible core at t=6ms.

5. Conclusions

In this paper, a higher-order global-local theory with a proposed algorithm for nonlinear dynamic analysis is presented for sandwich plates with embedded SMA wires. In the proposed algorithm, the Brinson model has been modified to simulate the nonsymmetric and symmetric behavior of SMA wires. This is important because, although in reality most of the SMAs have a non-symmetrical behavior between tension and compression, in most studies about composites or sandwich with embedded SMA wires during the last decades, SMA behavior in terms of tension and compression is considered the same due to the simplicity. But this assumption can lead to the formation of different hysteresis loops in wires, and as a result, it also affects the overall damping of the sandwich plate. Another advantage of the present study is the investigation of the phase transformation and martensite volume fraction of each point independently over the plate and continuously over time by using the proposed iterative algorithm. In this case, different points of the wires can have separate behaviors, for example, a point of the SMA wires can be at the local unloading status which the other point can be on loading and phase transformation stage.

The results showe that applying the assumption of symmetric SMA behavior reduces the stiffness of the sandwich plate and increases its transverse displacement. Also, due to the difference in the hysteresis loops formed in the SMA wires, the damping of the structure reduces when non-symmetric behavior of the wires is assumed in comparison to the symmetric behavior. However, it should be noted that this damping is more realistic and accurate. Finally, the results show that the higher-order global-local theory is an appropriate approach for investigating thick sandwich plate with embedded SMA wires. Using the presented theory will lead to desired results with the proper accuracy, along with the achievement of the appropriate solving time. On the other hand, in this paper, the transverse displacement of the core and its thickness changes are also simulated to be of great importance for the analysis of thick sandwich, especially with soft cores. The results show separate and independent behavior and different damping ratio of the upper and lower face sheets in a thick sandwich plate with a soft core. The mentioned difference proves the necessity of considering the deformation of the core in transverse direction.

References

[1] C. M. Wayman, and T. W. Duerig. "An introduction to martensite and shape memory" *Butterworth - Heinemann, Engineering Aspects of Shape Memory Alloys(UK)*, Vol. 22, No. 1, pp. 3-20, (1990).

[2] Liang, Chen, and Craig A. Rogers. "One-dimensional thermomechanical constitutive relations for shape memory materials." *Journal of intelligent material systems and structures*, Vol. 8, No. 4, pp. 285-302, (1997).

[3] Wilde, Krzysztof, Paolo Gardoni, and Yozo Fujino. "Base isolation system with shape memory alloy device for elevated highway bridges." *Engineering structures*, Vol. 22, No. 3, pp. 222-229, (2000).

[4] Gordaninejad, Faramarz, and Weida Wu. "A two-dimensional shape memory alloy/elastomer actuator." *International journal of solids and structures*, Vol. 38, No. 19, pp. 3393-3409, (2001).

[5] Epps, Jeanette, and Ramesh Chandra. "Shape memory alloy actuation for active tuning of composite beams." *Smart Materials and Structures*, Vol. 6, No. 3, p. 251, (1997).

[6] Lee, Hyo Jik, Jung Ju Lee, and Jeung Soo Huh. "A simulation study on the thermal buckling behavior of laminated composite shells with embedded shape memory alloy (SMA) wires." *Composite structures*, Vol. 47, No. 1, pp. 463-469, (1999).

[7] Lee, Hyo Jik, and Jung Ju Lee. "A numerical analysis of the buckling and postbuckling behavior of laminated composite shells with embedded shape memory alloy wire actuators." *Smart Materials and Structures*, Vol. 9, No. 6, p. 780, (2000).

[8] Rogers, Craig, and Daniel Barker, "Experimental studies of active strain energy tuning of adaptive composites." *31st Structures, Structural Dynamics and Materials Conference*. (1990).

[9] Park, Jae-Sang, Ji-Hwan Kim, and Seong-Hwan Moon. "Vibration of thermally post-buckled composite plates embedded with shape memory alloy fibers." *Composite Structures*, Vol. 63, No. 2, pp. 179-188, (2004).

[10] Ghomshei, M. M., et al. "Nonlinear transient response of a thick composite beam with shape memory alloy layers." *Composites Part B: Engineering*, Vol. 36, No.1, pp. 9-24, (2005).

[11] Brocca, M., L. C. Brinson, and Z. P. Bažant. "Three-dimensional constitutive model for shape memory alloys based on microplane model." *Journal of the Mechanics and Physics of Solids*, Vol. 50, No. 5, pp. 1051-1077, (2002).

[12] Shariyat, M., S. M. R. Khalili, and I. Rajabi. "A global–local theory with stress recovery and a new post-processing technique for stress analysis of asymmetric orthotropic sandwich plates with single/dual cores." *Computer Methods in Applied Mechanics and Engineering*, Vol. 286, pp. 192-215, (2015).

[13] Cunningham, P. R., R. G. White, and G. S. Aglietti. "The effects of various design parameters on the free vibration of doubly curved composite sandwich panels." *Journal of Sound and Vibration*, Vol. 230, No. 3, pp. 617-648, (2000).

[14] Masoud Tahani, and Asghar Nosier. "Free edge stress analysis of general cross-ply composite laminates under extension and thermal loading."*Composite Structures*, Vol. 60, No. 1, pp. 91-103, (2003).

[15] M. Shariyat, A generalized high-order global–local plate theory for nonlinear bending and buckling analyses of imperfect sandwich plates subjected to thermo-mechanical loads, *Composite Structures*, Vol. 92, No. 1, pp. 130-143, (2010).

[16] M. Shariyat, "A generalized global–local high-order theory for bending and vibration analyses of sandwich plates subjected to thermo-mechanical loads." *International Journal of Mechanical Sciences*, Vol. 52, No . 3, pp. 495-514, (2010).

[17] M. Shariyat, "Non-linear dynamic thermo-mechanical buckling analysis of the imperfect laminated and sandwich cylindrical shells based on a global-local theory inherently suitable for non-linear analyses". *International Journal of Non-Linear Mechanics*, Vol. 46, No. 1, pp. 253-271, (2011).

[18] M. Lezgy-Nazargah, M. Shariyat, SB. Beheshti-Aval "A refined high-order global-local theory for finite element bending and vibration analyses of the laminated composite beams". *Acta Mechanica*, Vol. 217, No. 3, pp. 219-242, (2011).

[19] J. L. Mantari, and C. Guedes Soares. "Generalized layerwise HSDT and finite element formulation for symmetric laminated and sandwich composite plates." *Composite Structures*, Vol. 105, pp. 319-331 (2013).

[20] M. Brocca, L. C. Brinson, and Z. P. Bažant, "Three-dimensional constitutive model for shape memory alloys based on microplane model." *Journal of the Mechanics and Physics of Solids.* Vol. 50, No. 5, pp. 1051-1077, (2002).

[21] A. Ghaznavi, M. Shariyat, Non-linear layerwise dynamic response analysis of sandwich plates with soft auxetic cores and embedded SMA wires experiencing cyclic loadings, *Composite Structures*, Vol. 171 pp. 185-197, (2017).

[22] M. Shariyat, A. Ghaznavi, "Influence analysis of phase transformation anisotropy of SMA wires embedded in sandwich plates with flexible cores by a third-order zigzag theory with dynamic 3D elasticity corrections". *Journal of Sandwich Structures and Materials*, Vol. 0, No. 0, pp. 1-46, (2018).

[23] M. Shariyat, A. Ghaznavi, "A one dimensional model for superelastic and shape memory effect of shape memory alloy with different elastic properties between austenite and martensite various complex loading", *Iranian Journal of*

Mechanical Engineering, Vol. 16, No. 1, 78-103, (2014).

[24] Yu I. Paskal, and L. Monasevich, "Hysteresis features of the martensitic transformation of titanium nickelide." *PHYS. METALS & METALLOG.* Vol. 52, No. 5, pp. 95-99, (1983).

[25] C. H. Thai, Loc V. Tran, Dung T. Tran, T. Nguyen-Thoi, H. Nguyen-Xuan. Analysis of laminated composite plates using higher-order shear deformation plate theory and node-based smoothed discrete shear gap method. *Applied Mathematical Modelling*, Vol. 36, pp. 5657-5677, (2012).

[26] Pagano, N. J. "Exact solutions for rectangular bidirectional composites and sandwich plates." *J. Composite Materials*, Vol. 4, pp. 20-34, (1970).

[27] Maenghyo Cho, and Oh Jinho. "Higher order zig-zag theory for fully coupled thermo- electric – mechanical smart

[28] composite plates." *International journal of solids and structures*, Vol. 41, No. 5, pp. 1331-1356, (2004).

[29] A. H., Sheikh, and A. Chakrabarti. "A new plate bending element based on higher-order shear deformation theory for the analysis of composite plates. "*Finite elements in analysis and design*, Vol. 39, No. 9, pp. 883-903, (2003).

[30] A. A., Khdeir, and J. N. Reddy. "Exact solutions for the transient response of symmetric cross-ply laminates using a higher-order plate theory."*Composites Science and Technology*, Vol. 34, No. 3, pp. 205-224, (1989).

How to cite this paper:

A. Ghaznavi, M. Shariyat, "Effects of asymmetric behavior of shape memory alloy on nonlinear dynamic responses of thick sandwich plates with embedded SMA wires", *Journal of Computational and Applied Research in Mechanical Engineering,* Vol. 9, No. 2, pp. 183-197, (2019).

DOI: 10.22061/jcarme.2019.2878.1300

URL: http://jcarme.sru.ac.ir/?_action=showPDF&article=1034